expanded coil conformation of the sort adopted by neutral polymers in good solvents may be reached in highly concentrated polyelectrolyte solutions without added salt.

Acknowledgment. We are grateful to an anonymous referee for helpful comments. This work was supported by NSF Grant DMB 88-16433.

References and Notes

(1) Mandel, M. *Eur. Polym. J.* **1983**, *19*, 911.
(2) Fuoss, R. M.; Katchalsky, A. *Proc. Natl. Acad. Sci. U.S.A.* **1951**, *37*, 579.
(3) Katchalsky, A. *Pure Appl. Chem.* **1971**, *26*, 327.
(4) Lifson, S.; Katchalsky, A. *J. Polym. Sci.* **1954**, *13*, 43.
(5) Marcus, R. A. *J. Chem. Phys.* **1955**, *23*, 1057.
(6) Alfrey, T., Jr.; Berg, P. W.; Morawetz, H. *J. Polym. Sci.* **1951**, *7*, 543.
(7) Manning, G. S. *J. Chem. Phys.* **1969**, *51*, 924.
(8) de Gennes, P. G.; Pincus, P.; Velasco, R. M.; Brochard, F. *J. Phys. (Les Ulis, Fr.)* **1976**, *37*, 1461.
(9) Odijk, T. *J. Polym. Sci., Polym. Phys. Ed.* **1977**, *15*, 477.
(10) Odijk, T.; Houwaart, A. C. *J. Polym. Sci., Polym. Phys. Ed.* **1978**, *16*, 627.
(11) Odijk, T. *Macromolecules* **1979**, *12*, 688.
(12) Bloomfield, V. A. In *Dynamic Light Scattering*; Pecora, R., Ed.; Plenum Press: New York, 1985; p 363.
(13) Schurr, J. M.; Schmitz, K. S. *Annu. Rev. Phys. Chem.* **1986**, *37*, 271.
(14) Koene, R. S.; Mandel, M. *Macromolecules* **1983**, *16*, 220.
(15) Koene, R. S.; Nicolai, T.; Mandel, M. *Macromolecules* **1983**, *16*, 227.
(16) Drifford, M.; Dalbiez, J. P. *J. Phys. Lett.* **1985**, *46*, L-311.
(17) Schmitz, K. S.; Yu, J. W. *Macromolecules* **1988**, *21*, 484.
(18) Grüner, F.; Lehmann, W. P.; Fahlbusch, H.; Weber, R. *J. Phys. A: Math. Gen.* **1981**, *18*, L307.
(19) Wang, L.; Yu, H. *Macromolecules* **1988**, *21*, 3498.
(20) Wang, L.; Yoon, H.; Yu, H. *Macromolecules*, in press.
(21) Wang, L.; Kim, S.; Shang, L.; Yu, H. *Macromolecules*, in press.
(22) Koene, R. S.; Nicolai, T.; Mandel, M. *Macromolecules* **1983**, *16*, 231.
(23) Noda, I.; Kato, N.; Kitano, T.; Nagasawa, M. *Macromolecules* **1981**, *14*, 668.
(24) Wang, L.; Bloomfield, V. A. *Macromolecules* **1989**, *22*, 2742.
(25) Wang, L.; Bloomfield, V. A. *Macromolecules*, in press.
(26) des Cloizeaux, J. *J. Phys. (Les Ulis, Fr.)* **1975**, *36*, 281.
(27) des Cloizeaux, J. *J. Phys. (Les Ulis, Fr.)* **1975**, *36*, 1199.
(28) Fixman, M.; Skolnick, J. *Macromolecules* **1978**, *11*, 863.
(29) Skolnick, J.; Fixman, M. *Macromolecules* **1977**, *10*, 944.
(30) Ise, N.; Okubo, T. *J. Am. Chem. Soc.* **1968**, *90*, 4527.
(31) Tondre, C.; Zana, R. *J. Phys. Chem.* **1972**, *76*, 3451.
(32) Reddy, M.; Marinsky, J. A. *J. Phys. Chem.* **1970**, *74*, 3884.
(33) Chu, P.; Marinsky, J. A. *J. Phys. Chem.* **1967**, *71*, 4352.
(34) Oman, S. *Makromol. Chem.* **1974**, *175*, 2133.
(35) Oman, S. *Makromol. Chem.* **1977**, *178*, 475.
(36) Takahashi, A.; Kato, N.; Nagasawa, M. *J. Phys. Chem.* **1970**, *74*, 944.
(37) Kozak, D.; Kristan, J.; Dolar, D. *Z. Phys. Chem. (Munich)* **1971**, *76*, 85.
(38) Vesnaver, G.; Skerjanc, J. *J. Phys. Chem.* **1986**, *90*, 4673.
(39) Koene, R. S.; Mandel, M. *Macromolecules* **1983**, *16*, 973.
(40) Aylward, N. N. *J. Polym. Sci., Polym. Chem. Ed.* **1970**, *8*, 909.
(41) Kotin, L.; Nagasawa, M. *J. Am. Chem. Soc.* **1961**, *83*, 1026.
(42) Bonner, O. D.; Overton, J. R. *J. Phys. Chem.* **1963**, *67*, 1035.
(43) Waxman, M. H.; Sundheim, B. R.; Gregor, H. P. *J. Phys. Chem.* **1953**, *57*, 969.
(44) Onsager, L. *Ann. N.Y. Acad. Sci.* **1949**, *51*, 627.
(45) Stigter, D. *Biopolymers* **1977**, *16*, 1435.
(46) Nierlich, M.; Boué, F.; Lapp, A.; Oberthur, R. *J. Phys. (Les Ulis, Fr.)* **1985**, *46*, 649.
(47) Callaghan, P.; Pinder, D. *Macromolecules* **1984**, *17*, 431.
(48) Kaji, K.; Urakawa, H.; Kanaya, T.; Kitamaru, R. *J. Phys. (Les Ulis, Fr.)* **1988**, *49*, 993.

Registry No. NaPSS, 9080-79-9; HPSS, 50851-57-5.

Hydrodynamic Interaction Effects on the Conformation of Flexible Chains in Simple Shear Flow

José J. López Cascales and José García de la Torre*

Departamento de Quimica Fisica, Universidad de Murcia, Espinardo 30100, Murcia, Spain.
Received April 4, 1989; Revised Manuscript Received July 21, 1989

ABSTRACT: The deformation of polymers modeled as bead-and-spring chains in simple shear flow is studied by Brownian dynamics simulation including hydrodynamic interaction (HI) effects. Previous theories neglecting HI, which are confirmed by our simulations, predicted that deformation scales with N^4, where N is the number of polymer units. Our results with nonpreaveraged HI give also an exponent of roughly 4, although the deformation is about half that predicted neglecting HI. Comparison with experimental data is made. We also discuss the utility of the dumbbell model for the representation of flexible polymers and the relative importance of spring stretching and alignment in the deformation of the chain.

Introduction

The theoretical study of the behavior of polymer chains under solvent flow presents difficulties, most of which are due to the hydrodynamic interaction (HI) between chain elements. Thus, it is usual to neglect hydrodynamic interaction effects in analytical calculation of rheological properties.[1] In some instances, hydrodynamic interactions can be introduced in an averaged form. Thus the theories are able to make qualitative or semiquantitative predictions that are quite useful. However, in some cases, the properties are quantitatively influenced, to a significant extent, by hydrodynamic interactions. In a recent paper,[2] we have shown that hydrodynamic interaction effects can be studied by computer simulation of the Brownian dynamics of the polymer chain in a flowing solvent.

In our previous study, we considered the most simple and common model in polymer rheology, the elastic dumbbell, in a simple shear flow. We evaluated, as a function of shear rate, the dumbbell extension, which mimics the end-to-end distance of the polymer molecule, and the components of the stress tensor. Apart from its evident influence on material properties, we detected that nonpreaveraged HI modified appreciably the square end-to-end

* To whom correspondence should be addressed.

0024-9297/90/2223-0809$02.50/0

Table I
Simulation Results for $\langle R^2 \rangle$ in the Absence of HI and Including HI with $h^* = 0.25$

$\dot{\gamma}$	N = 3	N = 4	N = 5	N = 8	N = 12	N = 20
			Without HI			
0	2.01 ± 0.02	2.98 ± 0.06	4.18 ± 0.08	7.27 ± 0.04	11.6 ± 0.2	22.0 ± 0.3
0.5	2.07 ± 0.03	3.14 ± 0.04	4.27 ± 0.08	8.9 ± 0.2	20.1 ± 0.2	175 ± 8
1.0	2.14 ± 0.06	3.25 ± 0.04	4.60 ± 0.04	12.8 ± 0.7	52 ± 2	722 ± 60
2.0	2.28 ± 0.01	3.76 ± 0.03	5.9 ± 0.2	28 ± 3	166 ± 3	1970 ± 70
3.0	2.46 ± 0.08	4.64 ± 0.08	8.5 ± 0.4	50 ± 5	378 ± 10	5000 ± 300
4.0	2.70 ± 0.03	5.77 ± 0.05	11.6 ± 0.1	95 ± 8	645 ± 20	8824 ± 600
5.0	2.96 ± 0.03	7.1 ± 0.3	16.3 ± 0.9	130 ± 10	956 ± 6	13800 ± 900
			With HI			
0	2.03 ± 0.06	2.94 ± 0.07	4.1 ± 0.1	7.0 ± 0.1	10.69 ± 0.06	19.0 ± 0.1
0.5	2.02 ± 0.05	3.02 ± 0.06	4.26 ± 0.06	7.47 ± 0.02	15.6 ± 0.1	56 ± 7
1.0	2.2 ± 0.1	3.26 ± 0.03	4.6 ± 0.1	9.2 ± 0.2	26.0 ± 0.5	176 ± 20
2.0	2.30 ± 0.05	3.7 ± 0.1	5.8 ± 0.2	17.3 ± 0.3	74 ± 3	1242 ± 100
3.0	2.70 ± 0.04	4.64 ± 0.04	7.7 ± 0.3	23.3 ± 0.3	160 ± 1	2684 ± 150
4.0	2.90 ± 0.03	5.65 ± 0.01	10.9 ± 0.1	48.1 ± 0.4	326 ± 13	4368 ± 650
5.0	3.5 ± 0.1	6.9 ± 0.2	12.0 ± 0.6	54 ± 3	470 ± 50	6700 ± 700

distance $\langle R^2 \rangle$, which was found to be about 25% larger than the value calculated in the absence of hydrodynamic interactions[3] when the shear rate was on the order of $\lambda_H = \zeta/4H$, where ζ is the friction coefficient of the beads and H is the force constant of the spring.

Here we report results obtained by Brownian dynamics simulation with nonpreaveraged HI for conformational averages of Gaussian bead-and-spring chains in simple shear flow. In addition to $\langle R^2 \rangle$, we investigate the different degree of extension of central and terminal springs and the averages of the angles between contiguous connector vectors. The influence of HI on these conformational aspects is considered. Studying such influence as a function of the number of chain elements, we arrive at some conclusions about the representativeness of the dumbbell model ($N = 2$) for polymer chains.

Methods

As in our previous paper, we have simulated Brownian trajectories of the polymer chain by means of the Ermak–McCammon algorithm,[4] which includes hydrodynamic interactions. A similar algorithm has been used recently by other authors.[5,6] The polymer model is simply a bead-and-spring chain with beads of radius σ and springs of root-mean-square length b. Excluded volume effects are neglected. Hydrodynamic interactions are represented by a Oseen tensor with an ad hoc modification for overlapping beads.[7] For the highest N's, the first-order Ermak–McCammon algorithm is somewhat slow, and we tried a second-order algorithm of the Runge–Kutta type, which is under development.[8] In the simulations, all the physical quantities are handled in dimensionless form, as in the previous paper. Thus, length is expressed in units of b, energy in units of kT where k is the Boltzmann constant and T is the absolute temperature, translational diffusion in units of kT/ζ, and time in units of $\zeta b^2/kT$. In this way we have (numerically) $b = 1$, $kT = 1$, $\zeta = 1$, H = 3, and $\lambda_H = 1/12$. In the case of simulations with hydrodynamic interactions we set the hydrodynamic interaction parameter $h^* = 0.25$, corresponding to $\sigma = 0.256$.

The size of the time steps in Brownian dynamics is critical. Δt must be as small as possible as required by the assumption that the diffusion matrix and the forces at the beads along the steps can be approximated by the initial value. A detailed study of the discretization of time has been described.[9] On the other hand, for a fixed number of steps, a large Δt gives longer trajectories that cover better the conformational space. After some trials, the time step in the simulations was finally set to $\Delta t = 0.01$ in reduced units. We observed that halving the time step had no appreciable influence on the final results. Typically, we generated four or five Brownian trajectories of about 5×10^4 steps each. At any rate, the validity of our working conditions is confirmed by the good agreement of the simulation values with some available theoretical results (vide infra). The final results are the means and standard deviations of the conformational averages evaluated for each subtrajectory.

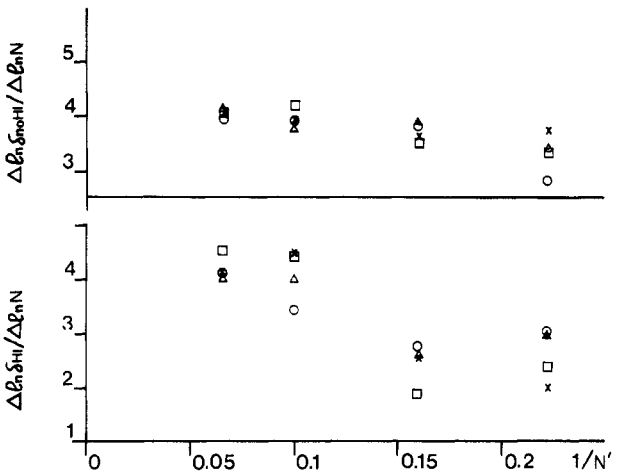

Figure 1. Deformation of the polymer coil, δ, obtained from the results in Table I, plotted versus $1/N$. (○) $\gamma = 2$; (□) $\gamma = 3$; (△) $\gamma = 4$; (×) $\gamma = 5$. The values of N used in this plot are such that their logarithms are the mean of those of the two N's used to evaluate δ as a ratio of finite differences.

Results and Discussion

Overall Dimensions. Simulations were carried out for chains up to $N = 20$ beads ($N - 1$ bonds) and shear rates up to $\dot{\gamma} = 5$ in reduced units. We report first the results obtained for the mean-squared end-to-end distance, $\langle R^2 \rangle$, and the mean-squared radius of gyration, $\langle S^2 \rangle$. Tables I and II contain the values obtained with and without HI. We also obtained a set of values in the absence of hydrodynamic interactions. The results without HI were found to be in very good agreement with the analytical result[3]

$$\langle R^2 \rangle_{noHI} = \langle R^2 \rangle_0 (1 + (1/45)N(N+1)(N^2+1)\lambda_H^2 \dot{\gamma}^2) \quad (1)$$

Table II
Simulation Results for $\langle S^2 \rangle$ in the Absence of HI and Including HI with $h^* = 0.25$

$\dot{\gamma}$	N = 3	4	5	8	12	20
			Without HI			
0	0.460 ± 0.005	0.650 ± 0.011	0.838 ± 0.008	1.372 ± 0.011	2.081 ± 0.009	3.7 ± 0.2
0.5	0.485 ± 0.005	0.67 ± 0.02	0.861 ± 0.012	1.62 ± 0.06	3.21 ± 0.04	23.0 ± 1.1
1.0	0.050 ± 0.010	0.691 ± 0.011	0.92 ± 0.02	2.09 ± 0.13	7.36 ± 0.18	85 ± 9
2.0	0.520 ± 0.005	0.772 ± 0.012	1.125 ± 0.003	4.28 ± 0.14	21.9 ± 0.5	252 ± 8
3.0	0.555 ± 0.005	0.90 ± 0.03	1.47 ± 0.02	7.6 ± 0.3	49.5 ± 1.3	630 ± 40
4.0	0.590 ± 0.005	1.061 ± 0.012	1.952 ± 0.005	13.1 ± 0.6	84 ± 4	1100 ± 80
5.0	0.640 ± 0.011	1.31 ± 0.03	2.65 ± 0.05	16.7 ± 0.9	124 ± 13	1700 ± 15
			With HI			
0	0.451 ± 0.012	0.623 ± 0.007	0.79 ± 0.05	1.31 ± 0.03	1.964 ± 0.006	3.32 ± 0.11
0.5	0.455 ± 0.005	0.64 ± 0.02	0.85 ± 0.03	1.386 ± 0.014	2.609 ± 0.018	7.9 ± 1.1
1.0	0.471 ± 0.009	0.67 ± 0.02	0.93 ± 0.03	1.57 ± 0.03	4.01 ± 0.04	23 ± 3
2.0	0.515 ± 0.015	0.751 ± 0.005	1.11 ± 0.03	2.71 ± 0.06	10.2 ± 0.4	119 ± 8
3.0	0.579 ± 0.005	0.89 ± 0.02	1.33 ± 0.05	3.33 ± 0.11	22.5 ± 0.7	353 ± 5
4.0	0.611 ± 0.005	1.057 ± 0.003	1.82 ± 0.08	6.57 ± 0.14	40.3 ± 1.0	568 ± 85
5.0	0.73 ± 0.03	1.27 ± 0.07	2.09 ± 0.03	7.3 ± 0.9	62.2 ± 1.5	860 ± 90

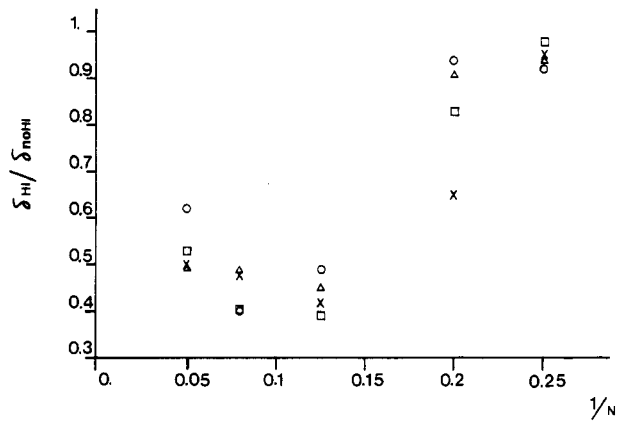

Figure 2. Ratios $\delta_{HI}/\delta_{noHI}$ versus $1/N$. The data points are as in Figure 1.

where $\langle R^2 \rangle_0 = (N-1)b^2$ is the value in the absence of flow ($\dot{\gamma} = 0$). Actually, the difference between the simulated values and those from eq 1 was 3% in the worst case (highest N and $\dot{\gamma}$) and always was smaller than the simulation uncertainty.

The polymer deformation can be measured by the relative increase, δ, in $\langle R^2 \rangle$:

$$\delta = \frac{\langle R^2 \rangle}{\langle R^2 \rangle_0} - 1 \tag{2}$$

Values of δ with and without HI are immediately obtained from the results listed in Table I. According to eq 1

$$\delta_{noHI} = (1/45)N(N+1)(N^2+1)\lambda_H^2\dot{\gamma}^2 \tag{3}$$

so that δ_{noHI} scales as $\dot{\gamma}^2$ for any N. From log–log plots of δ versus $\dot{\gamma}$, we found that the exponents for all the N's were between 1.9 and 2.0 both in the noHI case (in agreement with the theory) and in the HI case. Thus, the hydrodynamic interaction does not change the power-law dependence of the polymer deformation on shear rate.

We assume that if N is high enough, δ for fixed $\dot{\gamma}$ follows a scaling law:

$$\delta \propto N^{\alpha} \tag{4}$$

Indeed, eq 1 predicts $\alpha = 4$ for the noHI case. From our numerical results we estimate the exponent as $\alpha = d \ln \delta / d \ln N$. Actually the derivative was approximated by the quotient of finite differences, i.e.

$$\alpha \simeq (\ln \delta_2 - \ln \delta_1)/(\ln N_2 - \ln N_1) \tag{5}$$

δ_2 and δ_1 are the deformations corresponding to two values N_2 and N_1, respectively. Results of α obtained for discrete N's should converge to a limiting value for $N \to \infty$. The extrapolation to that limit is attempted in Figure 1, where the abscissa is $1/N'$, with $\ln N' = (\ln N_1 + \ln N_2)/2$. The individual values of α have a statistical uncertainty of up to ±0.5, so that this should be roughly the error of the limiting values.

The noHI values extrapolate clearly to $\alpha_{noHI} = 4$, in agreement with the theory for this case. The extrapolation in the HI case is more problematic because of the curvature (or undefined behavior) at low N and the large statistical errors in that region. Indeed, in a previous report of this work, in which we reached $N = 8$ only, we estimated a limiting α of about 2. Fortunately, the results seem to converge at high N. Thus, we have $\alpha = 4.1$, 4.5, 4.0, and 4.1 for $\dot{\gamma} = 2$, 3, 4, and 5 in the region of $N = 12$–20. It seem therefore reasonable to forecast that $\alpha_{HI} = 4$, i.e., so that the scaling law, eq 3, would be the same with and without hydrodynamic interactions.

In addition to $\langle R^2 \rangle$, the mean-squared radius of gyration, $\langle S^2 \rangle$ was used to characterize the conformation of the chains in the shear flow. The values obtained from the simulations are listed in Table II. The polymer deformation can also be expressed in terms of $\langle S^2 \rangle$. By analogy to eq 2 we define another deformation ratio

$$\beta = \frac{\langle S^2 \rangle}{\langle S^2 \rangle_0} - 1 \tag{6}$$

where

$$\langle S^2 \rangle_0 = \frac{(N-1)(N+1)b^2}{6N} \tag{7}$$

is the value in the absence of flow. A theoretical result[10,11] is available for the noHI case for high N

$$\beta_{noHI} = (16/945)N^4\lambda_H^2\dot{\gamma}^2 \quad (N \to \infty) \tag{8}$$

Our values for $N = 3$, 4, 5, 8, 12, and 20 agree within their statistical uncertainties with eq 8.

Our β_{HI} values were analyzed for their dependence on N and $\dot{\gamma}$ in the same manner as we did for δ_{HI}. As expected, β_{HI} scaled with $\dot{\gamma}^2$ and the exponent in N showed the same trend as before; the values found for $N = 12$–20 were 4.2 ± 0.5, 4.5 ± 0.4, 4.1 ± 0.1, and 4.1 ± 0.4 for $\dot{\gamma} = 2$, 3, 4, and 5, respectively. It seems that for $\langle S^2 \rangle$ the chain-length exponent is also 4.

As far as we know, there have not been many exhaustive investigations of the molecular weight dependence of the deformation of polymer chains in steady shear flows.

Table III
Ratio $\langle b_c^2\rangle/\langle b_t^2\rangle$ of Square Length of the Central Spring to That of the Terminal One

	N							
	4		8		12		20	
$\dot{\gamma}$	noHI	HI	noHI	HI	noHI	HI	noHI	HI
0.5	1.00 ± 0.03	1.00 ± 0.04	1.06 ± 0.02	1.000 ± 0.019	1.13 ± 0.02	1.06 ± 0.04	1.80 ± 0.04	1.18 ± 0.05
1.0	1.008 ± 0.017	1.01 ± 0.04	1.17 ± 0.02	1.00 ± 0.04	1.56 ± 0.04	1.22 ± 0.03	4.25 ± 0.16	1.84 ± 0.07
2.0	1.03 ± 0.03	1.02 ± 0.03	1.55 ± 0.07	1.21 ± 0.03	2.82 ± 0.07	1.75 ± 0.05	11.49 ± 0.14	4.08 ± 0.17
3.0	1.09 ± 0.05	1.04 ± 0.05	2.05 ± 0.11	1.17 ± 0.07	4.31 ± 0.14	2.57 ± 0.07	14.04 ± 0.07	11.2 ± 0.2
4.0	1.13 ± 0.04	1.12 ± 0.03	2.57 ± 0.10	1.72 ± 0.06	5.91 ± 0.19	3.09 ± 0.09	17.70 ± 0.10	13.22 ± 0.18
5.0	1.19 ± 0.05	1.11 ± 0.07	2.76 ± 0.11	1.55 ± 0.10	6.70 ± 0.08	4.57 ± 0.11	20.00 ± 0.10	17.2 ± 0.2

Table IV
Averages of the Cosines of Same Angles between Adjacent Bonds

	$\langle\cos\alpha_1\rangle$, $N = 3$		$\langle\cos\alpha_1\rangle$, $N = 8$		$\langle\cos\alpha_3\rangle$, $N = 8$		$\langle\cos\alpha_1\rangle$, $N = 20$		$\langle\cos\alpha_9\rangle$, $N = 20$	
$\dot{\gamma}$	noHI	HI	noHI	HI	noHI	HI	noHI	HI	noHI	HI
0	−0.036 ± 0.012	0.00 ± 0.03	0.027 ± 0.007	−0.005 ± 0.008	−0.018 ± 0.007	−0.02 ± 0.01	−0.032 ± 0.014	−0.101 ± 0.012	−0.011 ± 0.011	−0.022 ± 0.012
0.5	−0.048 ± 0.005	−0.02 ± 0.02	−0.03 ± 0.01	−0.01 ± 0.02	−0.002 ± 0.008	−0.01 ± 0.01	0.001 ± 0.012	0.001 ± 0.013	0.28 ± 0.03	0.08 ± 0.02
1.0	−0.036 ± 0.007	0.008 ± 0.018	0.01 ± 0.01	0.01 ± 0.02	0.08 ± 0.02	0.01 ± 0.01	0.10 ± 0.02	0.04 ± 0.02	0.53 ± 0.03	0.26 ± 0.04
2.0	−0.020 ± 0.005	0.010 ± 0.006	0.10 ± 0.01	0.06 ± 0.01	0.25 ± 0.02	0.13 ± 0.01	0.214 ± 0.013	0.13 ± 0.02	0.672 ± 0.012	0.47 ± 0.03
3.0	0.008 ± 0.006	0.05 ± 0.02	0.20 ± 0.02	0.11 ± 0.02	0.36 ± 0.02	0.16 ± 0.02	0.371 ± 0.012	0.26 ± 0.02	0.78 ± 0.02	0.62 ± 0.03
4.0	0.030 ± 0.009	0.067 ± 0.006	0.29 ± 0.01	0.20 ± 0.01	0.47 ± 0.02	0.32 ± 0.01	0.472 ± 0.012	0.33 ± 0.02	0.83 ± 0.02	0.71 ± 0.02
5.0	0.054 ± 0.009	0.07 ± 0.03	0.35 ± 0.02	0.20 ± 0.03	0.53 ± 0.02	0.30 ± 0.02	0.541 ± 0.017	0.41 ± 0.02	0.861 ± 0.012	0.74 ± 0.03

We are only aware of a recently published work[12] in which the shear-induced deformation of polystyrene in a good solvent was measured by small-angle neutron scattering. We guess that the excluded-volume effect on the scaling law for δ will surely be less important than that of hydrodynamic interactions.

Table II in ref 12 summarizes the experimental results. We neglect the data with high M and $\dot{\gamma}$ because a deviation from the scaling law $\beta \equiv \dot{\gamma}^2$ takes place (see Figure 10 in ref 12). By use of the data for $M = 1.7 \times 10^5$ with $\dot{\gamma} = 3000$ and 6000 s^{-1}, M = 2.92×10^5 with $\dot{\gamma} = 1500$ and 3000 s^{-1}, and $M = 3.09 \times 10^5$ with $\dot{\gamma} = 750$ and 1500 s^{-1}, a log–log plot of β versus MW gives $\alpha = 3.6 \pm 0.6$. Although the linear correlation is not high, the good agreement with theoretical and simulation results is significant.

It is evident from Tables I and II that HI has an important influence on the polymer dimensions. Assuming that both δ and β scale as $\dot{\gamma}^2 N^4$ ($N \to \infty$), the influence of HI can be characterized by the ratios $\delta_{HI}/\delta_{noHI}$. At high N, they coincide with $\langle R^2\rangle_{HI}/\langle R^2\rangle_{noHI}$ and $\langle S^2\rangle_{HI}/\langle S^2\rangle_{noHI}$. Results for the former are plotted versus $1/N$ in Figure 2, were we try to find the limiting ratio for $N \to \infty$. At high N the points seem to cluster near 0.5. The trend of β_{HI}/β_{noHI} is identical. Thus, the values of the ratio are 0.57 ± 0.05, 0.55 ± 0.12, 0.50 ± 0.11, and 0.51 ± 0.06 for $N = 20$ and $\dot{\gamma} = 2$, 3, 4, and 5. Although our simulations have an appreciable statistical uncertainty, we speculate that the limiting values of ratios could be equal to 1/2. Apart from the exact values of the ratios, it is evident that the polymer dimensions in shear flows calculated without HI are roughly twice those obtained when HI is considered in a rigorous, nonaveraged way.

This finding is relevant not only in regard to the importance of HI but also from the point of view of the validity of the dumbbell model for flexible polymer chains. In ref 2 we found that at moderately high $\dot{\gamma}$, $\langle R^2\rangle_{HI}$ was about 25% larger than $\langle R^2\rangle_{noHI}$. This corresponds to $\delta_{HI}/\delta_{noHI} \simeq 1.25$, in contrast with the values around 0.5 found now for chains. Thus the dumbbell model is misleading in the study of HI effects in polymer deformation in shear flow, since it predicts an effect that is incorrect not only quantitatively but also in its direction.

Stretching of Bonds and Angles. The elongation of a polymer chain in a flow can be regarded, in the context of the bead-and-spring model, as the composition of two simultaneous effects. One of them would be the stretching of the springs, which would represent the elongation of polymer subchains, and the other would correspond to the tendency to alignment of the end-to-end vectors of the subchains. The latter effect could be characterized by the statistics of the included angles.

In order to characterize the first effect, we have studied the average squared length of the bonds, denoted as $\langle b_i^2\rangle$, where $\mathbf{b}_i$ is the vector joining beads i and $i + 1$. One expects from physical intuition[13] that the central bond stretches in the flow much more than the terminal one. For elongational flow and assuming no hydrodynamic interaction, it has been shown[14] that the ratio of the mean-squared length of terminal bond to that of the central one scales as N^{-2}. We are not aware of similar predictions for shear flows, with or without HI. In Table III we report results from our Brownian dynamics simulation for the ratio $\langle b_c^2\rangle/\langle b_t^2\rangle$ where $\mathbf{b}_t^2$ is the mean of $\mathbf{b}_1^2$ and $\mathbf{b}_{N-1}^2$ and $\mathbf{b}_c^2$ is $\mathbf{b}_{N/2}^2$ if N is even or the mean of $\mathbf{b}_{(N-1)/2}^2$ and $\mathbf{b}_{(N+1)/2}^2$ if N is odd. Our results seem to indicate a week dependence of the ratio on the shear rate, although this could be a consequence of the short

length of the chains considered in our work. This circumstance and the appreciable simulation uncertainties prevent us from estimating a power law for the ratio. If the N^{-2} scaling would hold for shear flows with HI, the behavior that we observe for our short chains is far from it. Our most noticeable finding is that when the hydrodynamic interaction is included the ratios are remarkably smaller than those obtained in the absence of HI. We even forecast that the scaling law of the ratio with HI could be different than that without HI.

In regard to the second effect that causes the stretching of bead-and-spring chains, it can be detected in the angle α_i, with $i = 2, ..., N-1$, defined as the angle subtended by the directions of bonds $\mathbf{b}_{i-1}$ and $\mathbf{b}_i$. In Table IV we present values for the angle in a trimer and for the central and terminal angles when $N = 8$ and 20. We first note that the for the trimer $\langle \cos \alpha_1 \rangle \simeq 0$ and $\dot{\gamma}$ is as high as 5, a value for which $\langle R^2 \rangle$ is about 50% larger than $\langle R^2 \rangle_0$. Thus it seems that the primary contribution to the elongation of the model chain is the stretching of the springs rather than their alignment. The latter takes place at high shear rates and depends appreciably on N. We have made no attempt to characterize the N dependence of $\langle \cos \alpha_i \rangle$, but we notice from the results in Table IV that the central angles deformed in the shear flow more than the terminal ones and that hydrodynamic interaction effects make the deformation smaller than expected if interaction were absent. Thus our results including hydrodynamic interactions for varying N complement those from other analytical or simulation studies.[15,16]

Acknowledgment. We are grateful to A. Iniesta and F. G. Diaz for their help in many aspects of this work, which was supported by Grant PB87-0694 from the Comisión Interministerial de Ciencia y Tecnologá.

References and Notes

(1) Bird, R. B.; Hassager, O.; Armstrong, R. C.; Curtiss, C. F. Dynamics of Polymeric Liquids. *Kinetic Theory*; Wiley: New York, 1977; Vol. 2.
(2) Diaz, F. G.; García de la Torre, J.; Freire, J. J. *Polymer* **1989**, *30*, 259.
(3) Bird, R. B.; Saab, H. H.; Dotson, P. J.; Fan, X. J. *J. Chem. Phys.* **1983**, *79*, 5729.
(4) Ermak, D. L.; McCammon, J. A. *J. Chem. Phys.* **1978**, *69*, 1352.
(5) Zylka, W.; Öttinger, H. C. *J. Chem. Phys.* **1989**, *90*, 474.
(6) Liu, T. W. *J. Chem. Phys.* **1989**, *90*, 5826.
(7) Díaz, F. G.; Iniesta, A.; García de la Torre, J. *J. Chem. Phys.* **1987**, *87*, 6021.
(8) Iniesta, A.; Garcia de la Torre, J. *J. Chem. Phys.* **1990**, in press.
(9) Öttinger, H. C. *J. Non-Newtonian Fluid Mech.* **1986**, *19*, 357.
(10) Pistoor, N.; Binder, K. *Colloid Polym. Sci.* **1988**, *266*, 132.
(11) Frisch, H. L.; Pistoor, N.; Sariban, A.; Binder, K.; Fesjian, S. *J. Chem. Phys.* **1989**, *89*, 5194.
(12) Lindner, P.; Oberthur, R. C. *Colloid Polym. Sci.* **1988**, *266*, 886.
(13) Keller, A.; Odell, J. A. *Colloid Polym. Sci.* **1985**, *263*, 181.
(14) Rabin, Y. *J. Chem. Phys.* **1988**, *88*, 4014.
(15) Dotson, P. J. *J. Chem. Phys.* **1983**, *79*, 5730.
(16) Öttinger, H. C. *J. Chem. Phys.* **1986**, *84*, 1850.

Estimation of Free Volume for Gaseous Penetrants in Elastomeric Membranes by Monte Carlo Simulations

S. Trohalaki,† L. C. DeBolt,‡ and J. E. Mark*

Department of Chemistry and the Polymer Research Center, The University of Cincinnati, Cincinnati, Ohio 45221-0172

H. L. Frisch

Department of Chemistry, State University of New York at Albany, Albany, New York 12222. *Received March 8, 1989; Revised Manuscript Received July 3, 1989*

ABSTRACT: Theoretical aspects of the diffusion of small molecules in elastomeric polymer membranes are explored using a Monte Carlo simulation to estimate the free volume fraction in two typical siloxane elastomers. The model took into account the specific chemical structure of the polymer through the rotational isomeric state approximation. Calculated results for the two polymers agree semiquantitatively with experimentally determined diffusion coefficients.

Introduction

Membranes have found important industrial applications in the separation of gas mixtures. Such separations through rubbery polymer membranes is controlled by molecular diffusion of the penetrant molecules.[1,2] Fujita[2] has shown that the binary diffusion coefficient D is related to the free volume fraction f by

$$D(T,\phi) = A \exp[-B/f(T,\phi)] \quad (1)$$

where T is the absolute temperature, ϕ is the volume fraction of the penetrant gas, and A and B are constants. Evaluation of a polymer's free volume fraction is therefore useful in predicting its potential for gas separation. One way of doing this is by means of molecular simulations. We restrict our simulations here to siloxanes because they have the highest oxygen permeabilities among rubbery polymers.

† Current address: Department of Chemical Engineering and Materials Science, Syracuse University, Syracuse, NY 13244.
‡ Current address: Sherwin Williams Research Center, 10909 South Cottage Grove Avenue, Chicago, IL 60628.

0024-9297/90/2223-0813$02.50/0